


# 3-Manifold Triangulations with Small Treewidth

Kristóf Huszár 

Institute of Science and Technology Austria (IST Austria),  
Am Campus 1, 3400 Klosterneuburg, Austria  
kristof.huszar@ist.ac.at

Jonathan Spreer 

Institut für Mathematik, Freie Universität Berlin,  
Arnimallee 2, 14195 Berlin, Germany  
jonathan.spreer@fu-berlin.de

## Abstract

Motivated by fixed-parameter tractable (FPT) problems in computational topology, we consider the treewidth  $\text{tw}(M)$  of a compact, connected 3-manifold  $M$ , defined to be the minimum treewidth of the face pairing graph of any triangulation  $T$  of  $M$ . In this setting the relationship between the topology of a 3-manifold and its treewidth is of particular interest.

First, as a corollary of work of Jaco and Rubinstein, we prove that for any closed, orientable 3-manifold  $M$  the treewidth  $\text{tw}(M)$  is at most  $4g(M)-2$ , where  $g(M)$  denotes Heegaard genus of  $M$ . In combination with our earlier work with Wagner, this yields that for non-Haken manifolds the Heegaard genus and the treewidth are within a constant factor.

Second, we characterize all 3-manifolds of treewidth one: These are precisely the lens spaces and a single other Seifert fibered space. Furthermore, we show that all remaining orientable Seifert fibered spaces over the 2-sphere or a non-orientable surface have treewidth two. In particular, for every spherical 3-manifold we exhibit a triangulation of treewidth at most two.

Our results further validate the parameter of treewidth (and other related parameters such as cutwidth or congestion) to be useful for topological computing, and also shed more light on the scope of existing FPT-algorithms in the field.

**2012 ACM Subject Classification** Mathematics of computing → Geometric topology; Theory of computation → Fixed parameter tractability

**Keywords and phrases** computational 3-manifold topology, fixed-parameter tractability, layered triangulations, structural graph theory, treewidth, cutwidth, Heegaard genus, lens spaces, Seifert fibered spaces

**Digital Object Identifier** 10.4230/LIPIcs.SoCG.2019.44

**Related Version** A full version of this paper is available at <https://arxiv.org/abs/1812.05528>.

**Funding** *Kristóf Huszár*: Partially supported by the Einstein Foundation Berlin (grant EVF-2015-230) for his visits at Freie Universität Berlin.

*Jonathan Spreer*: Supported by grant EVF-2015-230 of the Einstein Foundation Berlin as well as by the DFG Collaborative Research Center SFB/TRR 109 “Discretization in Geometry and Dynamics”.

**Acknowledgements** We thank the developers of the free software *Regina* [11, 12] for creating a fantastic tool, and the anonymous reviewers for useful comments and suggestions regarding the exposition. KH thanks the people at the Discrete Geometry Group, Freie Universität Berlin, for their hospitality.

## 1 Introduction

Any given topological 3-manifold  $\mathcal{M}$  admits infinitely many combinatorially distinct triangulations  $\mathcal{T}$ , and the feasibility of a particular algorithmic task about  $\mathcal{M}$  might greatly depend on the choice of the input triangulation  $\mathcal{T}$ . Hence, it is an important question in



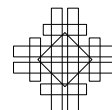
© Kristóf Huszár and Jonathan Spreer;  
licensed under Creative Commons License CC-BY  
35th International Symposium on Computational Geometry (SoCG 2019).

Editors: Gill Barequet and Yusu Wang; Article No. 44; pp. 44:1–44:20

Leibniz International Proceedings in Informatics



LIPICs Schloss Dagstuhl – Leibniz-Zentrum für Informatik, Dagstuhl Publishing, Germany



computational topology, how “well-behaved” a triangulation can be, taking into account “topological properties” of the underlying 3-manifold.

More concretely, there exist several algorithms in computational 3-manifold topology which solve inherently difficult (e.g., **NP**-hard) problems in linear time in the input size, once the input triangulation has a dual graph of bounded treewidth [13, 14, 15, 16, 32]. Such fixed-parameter tractable (FPT) algorithms are not only of theoretical importance but also provide practical tools: some of them are implemented in software packages such as *Regina* [11, 12] and, in selected cases, outperform previous state-of-the-art methods.

The presence of algorithms FPT in the treewidth of the dual graph of a triangulation immediately poses the following question. Given a 3-manifold  $\mathcal{M}$ , how small can the treewidth of the dual graph of a triangulation of  $\mathcal{M}$  be? This question has recently been investigated in a number of contexts, settling, for instance, that for some 3-manifolds there is no hope of finding triangulations with dual graphs of small treewidth [25] (see [17] for related work concerning the respective question about knots and their diagrams). Hyperbolic 3-manifolds nevertheless always admit triangulations of treewidth upper-bounded by their volume [31].

In this article we also focus on constructing small treewidth triangulations informed by the topological structure of a 3-manifold. To this end, we consider the notion of treewidth (cutwidth) of a 3-manifold as being the smallest treewidth (cutwidth) of a dual graph ranging over all triangulations thereof. The necessary background is introduced in Section 2.

In Section 3, building on [27], we show that the Heegaard genus dominates the cutwidth (and thus the treewidth as well) by virtue of the following statement.

► **Theorem 1.** *Let  $\mathcal{M}$  be a closed, orientable 3-manifold, and let  $\text{cw}(\mathcal{M})$  and  $\mathfrak{g}(\mathcal{M})$  respectively denote the cutwidth and the Heegaard genus of  $\mathcal{M}$ . We have  $\text{cw}(\mathcal{M}) \leq 4\mathfrak{g}(\mathcal{M}) - 2$ .*

Theorem 1, in combination with recent work by the authors and Wagner [25], implies that for the class of so-called non-Haken 3-manifolds, the Heegaard genus is in fact within a constant factor of both the cutwidth and the treewidth of a 3-manifold, providing an interesting connection between a classical topological invariant and topological properties directly related to the triangulations of a manifold. In Section 4, we further strengthen this link by looking at very small values of Heegaard genus and treewidth:

► **Theorem 2.** *The class of 3-manifolds of treewidth at most one coincides with that of Heegaard genus at most one together with the Seifert fibered space  $\text{SFS}[\mathbb{S}^2 : (2, 1), (2, 1), (2, -1)]$  of Heegaard genus two.*

In contrast, in Section 5 we show – by exhibiting treewidth two triangulations for all orientable Seifert fibered spaces over  $\mathbb{S}^2$  (Theorem 15) or a non-orientable surface (Theorem 16) – that linking Heegaard genus to treewidth fails to hold in general in a very strong sense: There are infinite families of 3-manifolds of unbounded Heegaard genus which are all of treewidth two (Corollary 21). Extending these observations we deduce that the treewidth of all 3-manifolds with spherical or  $\mathbb{S}^2 \times \mathbb{R}$  geometry equals two (Corollary 18).

Finally, combining these results, we determine the treewidth of 4889 out of the 4979 manifolds in the ( $\leq 10$ )-tetrahedra census (Table 1). Specifically, only 90 of them have treewidth possibly higher than two. These computations also confirm that not all minimal triangulations are of minimum treewidth (Corollary 20).

Altogether, our results and experiments further suggest that the treewidth of a 3-manifold is an interesting notion at the interface of topology and combinatorics which is well-suited to indicate the power of FPT algorithms in computational 3-manifold topology.

► **Remark 3.** The various triangulations described in Section 5 are available in form of a short *Regina* script [11, 12] in the full version of this article [24].

## 2 Preliminaries

### 2.1 Graphs

A *graph* (more precisely, a *multigraph*)  $G = (V, E)$  is an ordered pair consisting of a finite set  $V = V(G)$  of *nodes* and of a multiset  $E = E(G)$  of unordered pairs of nodes, called *arcs*.<sup>1</sup> A *loop* is an arc  $e \in E$  which is a multiset itself, e.g.,  $e = \{v, v\}$  for some  $v \in V$ . The *degree*  $\deg(v)$  of a node  $v \in V$  equals the number of arcs containing it, counted with multiplicity. If all of its nodes have the same degree  $k \in \mathbb{N}$ , a graph is called *k-regular*. A *tree* is a connected graph with  $n$  nodes and  $n - 1$  arcs. The term *leaf* denotes a node of degree one.

For general background on graph theory we refer to [19].

**Treewidth.** Originating from graph minor theory [29] and central to parametrized complexity [20, Part III], treewidth [5, 7, 41] measures the similarity of a given graph to a tree. More precisely, a *tree decomposition* of  $G = (V, E)$  is a pair  $(\{B_i : i \in I\}, T = (I, F))$  with *bags*  $B_i \subseteq V$ ,  $i \in I$ , and a tree  $T = (I, F)$ , such that a)  $\bigcup_{i \in I} B_i = V$ , b) for every arc  $\{u, v\} \in E$ , there exists  $i \in I$  with  $\{u, v\} \subseteq B_i$ , and c) for every  $v \in V$ ,  $T_v = \{i \in I : v \in B_i\}$  spans a connected subtree of  $T$ . The *width* of a tree decomposition equals  $\max_{i \in I} |B_i| - 1$ , and the *treewidth*  $\text{tw}(G)$  is the smallest width of any tree decomposition of  $G$ .

On one hand, treewidth is useful in the analysis of algorithms [8]. On the other hand, congestion (also known as carving-width) and cutwidth have recently turned out to be helpful mediators to connect treewidth with classical topological invariants [17, 25, 31]. In this work, alongside with treewidth, we also work with cutwidth.

**Cutwidth.** Consider an ordering  $(v_1, \dots, v_n)$  of  $V$ . The set  $C_\ell = \{\{v_i, v_j\} \in E : i \leq \ell < j\}$ , where  $1 \leq \ell < n$ , is called a *cutset*. The *width* of the ordering is the size of the largest cutset. The *cutwidth* [18], denoted by  $\text{cw}(G)$ , is the minimum width over all orderings of  $V$ .

### 2.2 Triangulations and Heegaard splittings of 3-manifolds

The main objects of study in this article are *3-manifolds*, i.e., topological spaces in which every point has a neighborhood homeomorphic to  $\mathbb{R}^3$  or to the closed upper half-space  $\{(x, y, z) \in \mathbb{R}^3 : z \geq 0\}$ . For a 3-manifold  $\mathcal{M}$ , its *boundary*  $\partial\mathcal{M}$  consists of all points of  $\mathcal{M}$  not having a neighborhood homeomorphic to  $\mathbb{R}^3$ . A 3-manifold is *closed* if it is compact and has an empty boundary. Two 3-manifolds are considered equivalent if they are homeomorphic. We refer to [44] for an introduction to 3-manifolds (cf. [22], [23], [26] and [48]), and to [42, Lecture 1] for an overview of the key concepts defined in this subsection.

All 3-manifolds considered in this paper are compact and orientable.

**Triangulations.** In the field of computational topology, a 3-manifold is often presented as a *triangulation* [4, 34], i.e., a finite collection of abstract tetrahedra “glued together” by identifying pairs of their triangular faces called *triangles*. Due to these *face gluings*, several tetrahedral edges (or vertices) are also identified and we refer to the result as a single *edge (or vertex) of the triangulation*. The face gluings, however, cannot be arbitrary. For a triangulation  $\mathcal{T}$  to describe a closed 3-manifold, it is necessary and sufficient that no

<sup>1</sup> Throughout the article, the terms *edge* and *vertex* denote an edge or vertex of a triangulated surface or 3-manifold, while the words *arc* and *node* refer to an edge or vertex in a graph.

tetrahedral edge is identified with itself in reverse, and the boundary of a small neighborhood around each vertex is  $\mathbb{S}^2$ , a 2-sphere. If, in addition, the boundaries of small neighborhoods of some of the vertices are disks, then  $\mathcal{T}$  describes a 3-manifold with boundary.

To study a triangulation  $\mathcal{T}$ , it is often useful to consider its *dual graph*  $\Gamma(\mathcal{T})$ , whose nodes and arcs correspond to the tetrahedra of  $\mathcal{T}$  and to the face gluings between them, respectively. By construction,  $\Gamma(\mathcal{T})$  is a multigraph with maximum degree  $\leq 4$ .

**Heegaard splittings.** *Handlebodies*, which can be thought of as thickened graphs, provide another way to describe 3-manifolds. A *Heegaard splitting* [43] is a decomposition  $\mathcal{M} = \mathcal{H} \cup_f \mathcal{H}'$ , where we start with the disjoint union of two homeomorphic handlebodies,  $\mathcal{H}$  and  $\mathcal{H}'$  and then identify their boundary surfaces via a homeomorphism  $f: \partial\mathcal{H} \rightarrow \partial\mathcal{H}'$  referred to as the *attaching map*. Every closed, compact, and orientable 3-manifold  $\mathcal{M}$  can be obtained this way. Moreover, we may assume, without loss of generality, that  $f$  is orientation-preserving. The smallest genus of a boundary surface ranging over all Heegaard splittings of  $\mathcal{M}$ , denoted by  $\mathfrak{g}(\mathcal{M})$ , is called the *Heegaard genus* of  $\mathcal{M}$ . Heegaard splittings with isotopic attaching maps yield homeomorphic 3-manifolds, hence are considered equivalent.

### 2.3 Orientable Seifert fibered spaces

Seifert fibered spaces, see [46], comprise an important class of 3-manifolds. Here we describe the orientable ones following [42] (cf. [22, Sec. 2.1], [26, Ch. VI], [35], [36], or [44, Sec. 3.7]).

Let us consider the surface  $\mathcal{F}_{g,r} = \mathcal{F}_g \setminus (\text{int } D_1 \cup \dots \cup \text{int } D_r)$  obtained from the closed orientable genus  $g$  surface by removing the interiors of  $r$  pairwise disjoint disks. Taking the product with the circle  $\mathbb{S}^1$  yields an orientable 3-manifold  $\mathcal{F}_{g,r} \times \mathbb{S}^1$  whose boundary consists of  $r$  tori; namely,  $\partial(\mathcal{F}_{g,r} \times \mathbb{S}^1) = (\partial D_1) \times \mathbb{S}^1 \cup \dots \cup (\partial D_r) \times \mathbb{S}^1$ . For each  $(\partial D_i) \times \mathbb{S}^1$ ,  $1 \leq i \leq r$ , we glue in a solid torus so that its meridian wraps  $a_i$  times around the meridian  $(\partial D_i) \times \{y_i\}$  and  $b_i$  times around the longitude  $\{x_i\} \times \mathbb{S}^1$  of  $(\partial D_i) \times \mathbb{S}^1$ . Here  $a_i$  and  $b_i$  are assumed to be coprime integers with  $a_i \geq 2$ , and the point  $(x_i, y_i) \in (\partial D_i) \times \mathbb{S}^1$  is chosen arbitrarily. This way we obtain a closed orientable 3-manifold  $\mathcal{M} = \text{SFS}[\mathcal{F}_g : (a_1, b_1), \dots, (a_r, b_r)]$  which is called the *Seifert fibered space over  $\mathcal{F}_g$  with  $r$  exceptional (or singular) fibers*. In relation to  $\mathcal{M}$ , the surface  $\mathcal{F}_g$  is referred to as the *base space* (or *orbit surface*).

► **Example 4.** *Lens spaces*, the 3-manifolds of Heegaard genus one, coincide with Seifert fibered spaces over  $\mathbb{S}^2$  having at most one (or two, cf. [42, p. 27]) exceptional fiber(s).<sup>2</sup>

**Non-orientable base spaces.** With a slight modification of the above construction, one can obtain additional orientable Seifert fibered spaces having non-orientable base spaces. Beginning with  $\mathcal{N}_g$ , the non-orientable genus  $g$  surface, we pass to  $\mathcal{N}_{g,r}$  by adding  $r$  punctures (i.e., by removing  $r$  pairwise disjoint open disks). At this point, however, instead of taking the product  $\mathcal{N}_{g,r} \times \mathbb{S}^1$  (which yields a non-orientable 3-manifold) we consider the “orientable  $\mathbb{S}^1$ -bundle” over  $\mathcal{N}_{g,r}$ , which has again  $r$  torus boundary components. As before, we conclude by gluing in  $r$  solid tori, specified by pairs of coprime integers  $(a_i, b_i)$  with  $a_i \geq 2$ , where  $1 \leq i \leq r$ . The notation for the resulting 3-manifold remains the same.

See [30, Section 2] for a concrete and detailed description of Seifert fibered spaces both over orientable and non-orientable surfaces (cf. the classes  $\{Oo, g\}$  and  $\{On, g\}$  therein).

<sup>2</sup> In particular, we regard  $\mathbb{S}^2 \times \mathbb{S}^1$  (the SFS over  $\mathbb{S}^2$  without exceptional fibers) to be a lens space as well.

**Geometric structures on 3-manifolds.** The significance of Seifert fibered spaces is exemplified by their role in the geometrization of 3-manifolds – a celebrated program initiated by Thurston [47], influenced by Hamilton [21], and completed by Perelman [37, 39, 38], cf. [3, 28, 33, 40] – as they account for six out of the eight possible “model geometries” [45] the building blocks may admit in the “canonical decomposition” of a closed 3-manifold.

### 3 The treewidth of a 3-manifold

In this section we prove Theorem 1. For this, we first recall how to turn graph-theoretical parameters, such as treewidth or cutwidth, into topological invariants of 3-manifolds. This is followed by a very brief and selective introduction to the theory *layered triangulations* as defined by Jaco and Rubinstein [27]. We then present the proof of Theorem 1 which, on the topological level, is a direct consequence of this theory, and conclude with a remark on some practical aspects derived from the constructive nature of the proof.

#### 3.1 Topological invariants from graph parameters

Recall the notions of treewidth and cutwidth from Section 2.1.

► **Definition 5.** Let  $\mathcal{M}$  be a 3-manifold and let  $\mathcal{T}$  be a triangulation of  $\mathcal{M}$ . By the treewidth of  $\mathcal{T}$  we mean  $\text{tw}(\Gamma(\mathcal{T}))$ , i.e., the treewidth of its dual graph, and the treewidth  $\text{tw}(\mathcal{M})$  of  $\mathcal{M}$  is defined to be the smallest treewidth of any triangulation of  $\mathcal{M}$ . In other words,

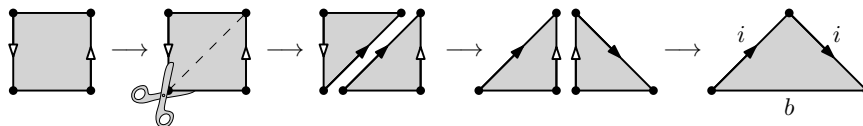
$$\text{tw}(\mathcal{M}) = \min\{\text{tw}(\Gamma(\mathcal{T})) : \mathcal{T} \text{ is a triangulation of } \mathcal{M}\}. \quad (1)$$

The definition of *cutwidth*  $\text{cw}(\mathcal{M})$  is analogous. Using [6, Theorems 47 and 49] it follows that  $\text{tw}(\mathcal{M}) \leq \text{cw}(\mathcal{M})$ . Complementing Definition 5, we note that there are simple arguments proving that any 3-manifold admits triangulations of arbitrarily high treewidth (cf. [24]).

#### 3.2 Layered triangulations

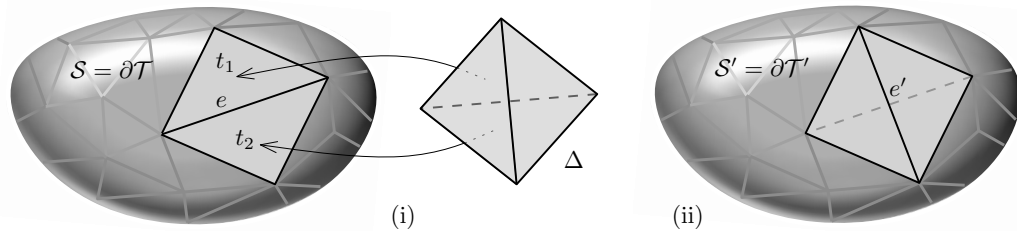
The theory of layered triangulations of 3-manifolds, due to Jaco and Rubinstein [27], captures the inherently topological notion of a Heegaard splitting, see Section 2.2, in a combinatorial way. Here we outline the terminology important for our purposes. Despite all the technicalities, the nomenclature is very expressive and encapsulates much of the intuition.

**Spines and layerings.** Let  $\mathcal{N}_{g,r}$  denote the non-orientable surface of genus  $g$  with  $r$  punctures (i.e., boundary components). A  $g$ -spine is a 1-vertex triangulation of  $\mathcal{N}_{g,1}$ . It has one vertex,  $3g - 1$  edges (out of which  $3g - 2$  are interior and one is on the boundary), and  $2g - 1$  triangles. In particular, the Euler characteristic of any  $g$ -spine equals  $1 - g$ .



■ **Figure 1** Transforming the (well-known depiction of the) Möbius band – the non-orientable surface of genus one with one puncture – into a 1-spine with interior edge  $i$ .

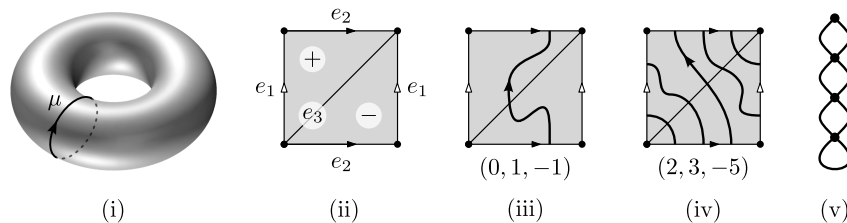
Now consider a triangulation  $\mathcal{S}$  of a surface – usually seen as a  $g$ -spine or as the boundary of a triangulated 3-manifold – and let  $e$  be an interior edge of  $\mathcal{S}$  with  $t_1$  and  $t_2$  being the two triangles of  $\mathcal{S}$  containing  $e$ . Gluing a tetrahedron  $\Delta$  along  $t_1$  and  $t_2$  without a twist is called a *layering* onto the edge  $e$  of the surface  $\mathcal{S}$ , cf. Figure 2(i). Importantly, we allow  $t_1$  and  $t_2$  to coincide, e.g., when layering on the interior edge of a 1-spine (Figure 1, right).



■ **Figure 2** (i) Layering onto the edge  $e$  of  $\mathcal{S} = \partial\mathcal{T}$ , (ii) which has the effect of “flipping”  $e$ .

**Layered handlebodies.** It is a pleasant fact that by layering a tetrahedron onto each of the  $3g - 2$  interior edges of a  $g$ -spine we obtain a triangulation of the genus  $g$  handlebody  $\mathcal{H}_g$ , called a *minimal layered triangulation* thereof (see Figure 4). More generally, we call any triangulation obtained by additional layerings a *layered triangulation* of  $\mathcal{H}_g$  [26, Section 9].

The case  $g = 1$  is of particular importance. Starting with a 1-spine (Figure 1) and layering on its interior edge  $i$  produces a 1-tetrahedron triangulation  $\mathcal{T}$  of the solid torus  $\mathcal{H}_1$  ([24]). Its boundary  $\mathcal{S} = \partial\mathcal{T}$  is the unique 2-triangle triangulation of the torus with one vertex and three edges, and layering onto any edge of  $\mathcal{S}$  yields another triangulation of  $\mathcal{H}_1$ . We may iterate this procedure to obtain further triangulations, any of which we call a *layered solid torus* (cf. [10, Section 1.2] for a detailed exposition). By construction, its dual graph consists of a single loop at the end of a path of double arcs; see, e.g, Figure 3(v).



■ **Figure 3**

While combinatorially the same, boundary triangulations of layered solid tori generally are not isotopic; they can be described as follows. Consider a “reference torus”  $\mathbb{T}$  with a fixed meridian  $\mu$ , Figure 3(i). Given a layered solid torus, its boundary induces a triangulation of  $\mathbb{T}$ . Label the two triangles with  $+$  and  $-$ , and the three edges with  $e_1, e_2$ , and  $e_3$ , Figure 3(ii); and orientation of  $\mu$ . Let  $p, q$  and  $r$  denote the geometric intersection number of  $\mu$  with  $e_1, e_2$  and  $e_3$ , respectively. We say that the corresponding layered solid torus is of type  $(p, q, r)$ , or  $\text{LST}(p, q, r)$  for short. See, e.g., Figure 3(iii)–(iv).

It can be shown that  $p, q, r$  are always coprime with  $p + q + r = 0$ . Conversely, for any such triplet, one can construct a layered solid torus of type  $(p, q, r)$ , cf. [10, Algorithm 1.2.17].

**Layered 3-manifolds.** Let  $\mathcal{M}$  be a closed, orientable 3-manifold given via a Heegaard splitting  $\mathcal{M} = \mathcal{H} \cup_f \mathcal{H}'$ . If  $\mathcal{H}$  and  $\mathcal{H}'$  can be endowed with layered triangulations  $\mathcal{T}$  and  $\mathcal{T}'$ , respectively, such that the attaching map  $f$  is simplicial, then the union  $\mathcal{T} \cup_f \mathcal{T}'$  triangulates  $\mathcal{M}$  and is called a *layered triangulation* of  $\mathcal{M}$ . The next theorem is fundamental.

► **Theorem 6** (Jaco–Rubinstein, Theorem 10.1 of [27]). *Every closed, orientable 3-manifold admits a layered triangulation (which is a one-vertex triangulation by construction).*

### 3.3 Treewidth versus Heegaard genus

In [25, Theorem 4] it was shown that for a closed, orientable, irreducible, non-Haken (cf. [25, Section 2.2]) 3-manifold  $\mathcal{M}$ , the Heegaard genus  $\mathfrak{g}(\mathcal{M})$  and the treewidth  $\text{tw}(\mathcal{M})$  satisfy

$$\mathfrak{g}(\mathcal{M}) < 24(\text{tw}(\mathcal{M}) + 1). \quad (2)$$

In this section we further explore the connection between these two parameters, guided by two questions: **1.** Does a reverse inequality hold? **2.** Can one refine the assumptions?

For the first one, we give an affirmative answer (Theorem 1). The result is almost immediate if one inspects a layered triangulation of a closed, orientable 3-manifold. Due to work of Jaco and Rubinstein, this approach is always possible (cf. Theorem 6).

The second question is more open-ended. As a first step, we observe the following.

► **Proposition 7.** *There exists an infinite family of 3-manifolds of bounded cutwidth – hence of bounded treewidth – with unbounded Heegaard genus.*

This follows from the fact that, while Heegaard genus is additive under taking connected sums, cutwidth essentially is not affected by this operation, see the full version [24].

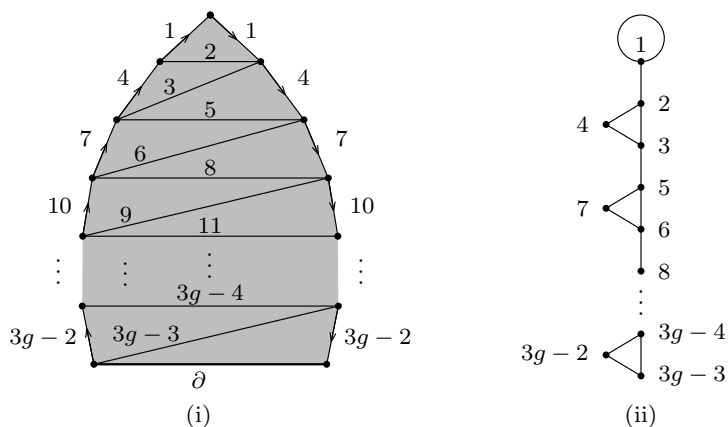
► **Remark 8.** Proposition 7 shows that among reducible 3-manifolds one can easily find infinite families which violate (2). Nevertheless, irreducibility alone is insufficient for (2) to hold. In particular, in Section 5 we prove that orientable Seifert fibered spaces over  $\mathbb{S}^2$  have treewidth at most two (Theorem 15). However, all but two of them are irreducible [44, Theorem 3.7.17] and they can have arbitrarily large Heegaard genus [9, Theorem 1.1].

Recent work of de Mesmay, Purcell, Schleimer, and Sedgwick [17] suggests that one might be able to obtain an inequality similar to (2) for (closed) Haken manifolds as well, by imposing appropriate conditions on the (incompressible) surfaces they contain.

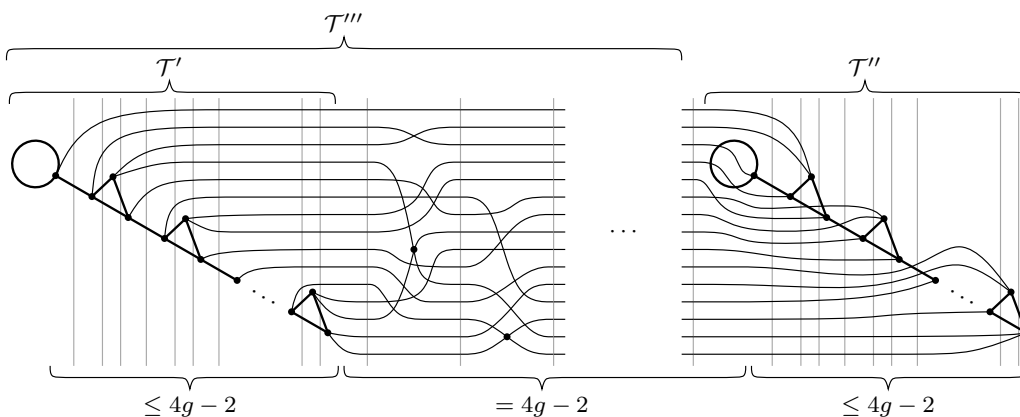
Nevertheless, as mentioned before, a reverse inequality always holds. In order to establish that, we utilize layered triangulations. See Section 3.2 for a brief introduction.

**Proof of Theorem 1.** Let  $g = \mathfrak{g}(\mathcal{M})$ . Consider the  $g$ -spine  $S$  in Figure 4(i) together with the indicated order in which we layer onto the  $3g - 2$  interior edges of  $S$  to build two copies  $\mathcal{T}'$  and  $\mathcal{T}''$  of a minimal layered triangulation of the genus  $g$  handlebody. See Figure 4(ii) for the dual graph of  $\mathcal{T}'$  (and of  $\mathcal{T}''$ ). Note that  $\partial\mathcal{T}'$  and  $\partial\mathcal{T}''$  consist of  $4g - 2$  triangles each.

By Theorem 6, we may extend  $\mathcal{T}'$  to a layered triangulation  $\mathcal{T}'''$  which can be glued to  $\mathcal{T}''$  along a simplicial map  $f : \partial\mathcal{T}''' \rightarrow \partial\mathcal{T}''$  to yield a triangulation  $\mathcal{T} = \mathcal{T}''' \cup_f \mathcal{T}''$  of  $\mathcal{M}$ . This construction imposes a natural ordering on the tetrahedra of  $\mathcal{T}$ : **1.** Start by ordering the tetrahedra of  $\mathcal{T}'$  according to the labels of the edges of  $S$  onto which they are initially layered. **2.** Continue with all tetrahedra between  $\mathcal{T}'$  and  $\mathcal{T}''$  in the order they are attached to  $\mathcal{T}'$  in order to build up  $\mathcal{T}'''$ . **3.** Finish with the tetrahedra of  $\mathcal{T}''$  again in the order of the labels of the edges of  $S$  onto which they are layered. This way we obtain a linear layout of the nodes of  $\Gamma(\mathcal{T})$  which realizes width  $4g - 2$  (Figure 5). Therefore  $\text{cw}(\mathcal{M}) \leq 4g - 2$ . ◀



■ **Figure 4** A  $g$ -spine  $S$  together with the order in which we layer onto its interior edges (i), and the dual graph of resulting minimal layered triangulation of the genus  $g$  handlebody (ii).



■ **Figure 5** A linear layout showing that  $\text{cw}(\mathcal{M})$  is bounded above by  $4\mathfrak{g}(\mathcal{M}) - 2$ .

Combining Theorem 1 with  $\text{tw}(\mathcal{M}) \leq \text{cw}(\mathcal{M})$ , we directly deduce the following.

► **Corollary 9.** *For any closed, orientable, irreducible, non-Haken 3-manifold  $\mathcal{M}$  the Heegaard genus  $\mathfrak{g}(\mathcal{M})$  and the treewidth  $\text{tw}(\mathcal{M})$  satisfy*

$$\frac{1}{4} \text{tw}(\mathcal{M}) + 2 \leq \mathfrak{g}(\mathcal{M}) < 24(\text{tw}(\mathcal{M}) + 1). \tag{3}$$

In [1, Question 5.3] the authors ask whether computing the Heegaard genus of a 3-manifold is still hard when restricting to the set of non-Haken 3-manifolds. Corollary 9 implies that the answer to this question also has implications on the hardness of computing or approximating the treewidth of non-Haken manifolds.

### 3.4 An algorithmic aspect of layered triangulations

Layered triangulations are intimately related to the rich theory of surface homeomorphisms, and in particular the notion of the mapping class group. Making use of this connection, as well as some very useful results due to Bell [2], we present a general algorithmic method to turn a 3-manifold  $\mathcal{M}$ , given by a small genus Heegaard splitting in some reasonable way, into a triangulation of  $\mathcal{M}$  while staying in full control over the size of this triangulation.



Namely, if  $\mathcal{M}$  is given by a genus  $g$  Heegaard splitting with the attaching map presented as a word  $w$  over a set of Dehn twists  $X$  generating the genus  $g$  mapping class group, then there exists a constant  $K(g)$  such that we can construct a layered triangulation of  $\mathcal{M}$  of size  $O(K(g)|w|)$ , cutwidth  $\leq 4g - 2$ , in time  $O(K(g)(|X| + |w|))$ .

See the full version of this article [24] for the definition of all notions underlying this observation, a precise formulation of the above statement, and a proof.

**4 3-Manifolds of treewidth at most one**

This section is dedicated to the proof of Theorem 2. As the treewidth is not sensitive to multiple arcs or loops, it is helpful to also consider *simplifications* of multigraphs, in which we forget about loops and reduce each multiple arc to a single one (Figure 6).

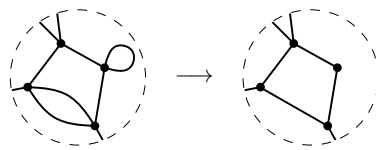


**Figure 6** The local effect of simplification in a multigraph.

One direction in Theorem 2 immediately follows from work of Jaco and Rubinstein.

► **Theorem 10** (cf. Theorem 6.1 of [27]). *Every lens space admits a layered triangulation  $\mathcal{T}$  with the simplification of  $\Gamma(\mathcal{T})$  being a path. In particular, all 3-manifolds of Heegaard genus at most one have treewidth at most one.*

For the proof of the other direction, the starting point is the following observation.

► **Lemma 11.** *If the simplification of a 4-regular multigraph  $G$  is a tree, then it is a path.*

**Proof.** Let  $S(G)$  denote the simplification of  $G$ . Call an arc of  $S(G)$  *even* (resp. *odd*) if its corresponding multiple arc in  $G$  consist of an even (resp. odd) number of arcs. Let  $Odd(G)$  be the subgraph of  $S(G)$  consisting of all odd arcs. It follows from a straightforward parity argument that all nodes in  $Odd(G)$  have an even degree. In particular, if the set  $E(Odd(G))$  of arcs is nonempty, then it necessarily contains a cycle. However, this cannot happen as  $S(G)$  is a tree by assumption. Consequently, all arcs of  $S(G)$  must be even. This implies that every node of  $S(G)$  has degree at most 2 (otherwise there would be a node in  $G$  with degree  $> 4$ ), which in turn implies that  $S(G)$  is a path. ◀

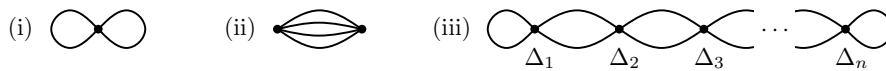


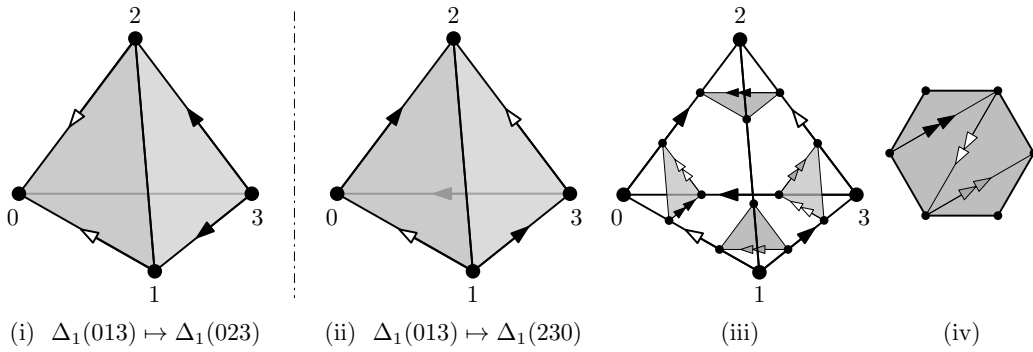
**Figure 7** The only possible dual graphs (corresp. to closed 3-manifolds) of treewidth at most one.

Consequently, if  $tw(\Gamma(\mathcal{T})) \leq 1$  for a triangulation  $\mathcal{T}$  of a closed 3-manifold, then  $\Gamma(\mathcal{T})$  is a “thick” path. If  $tw(\Gamma(\mathcal{T})) = 0$ , then  $\Gamma(\mathcal{T})$  is a single node with two loops (Figure 7(i)). By looking at the *Closed Census* [12], the only orientable 3-manifolds admitting a dual graph of this kind are  $\mathbb{S}^3$  and two lens spaces. If  $\Gamma(\mathcal{T})$  has a quadruple arc, then it must be a path of length two (Figure 7(ii)), and the only 3-manifold not a lens space appearing here is  $SFS[\mathbb{S}^2 : (2, 1), (2, 1), (2, -1)]$  which has Heegaard genus two, cf. [42, p. 27]. Otherwise, order the tetrahedra  $\Delta_1, \dots, \Delta_n$  of  $\mathcal{T}$  as shown in Figure 7(iii), and define  $\mathcal{T}_i \subset \mathcal{T}$  to be the  $i^{th}$  subcomplex of  $\mathcal{T}$  consisting of  $\Delta_1, \dots, \Delta_i$ .

$\mathcal{T}_1$  is obtained by identifying two triangles of  $\Delta_1$ . Without loss of generality, we may assume that these are the triangles  $\Delta_1(013)$  and  $\Delta_1(023)$ . A priori, there are six possible face gluings between them (corresponding to the six bijections  $\{0, 1, 2\} \rightarrow \{0, 2, 3\}$ ).

The gluing  $\Delta_1(013) \mapsto \Delta_1(023)$  yields a 3-vertex triangulation of the 3-ball, called a *snapped 3-ball*, and is an admissible choice for  $\mathcal{T}_1$ , Figure 8(i).  $\Delta_1(013) \mapsto \Delta_1(032)$  and  $\Delta_1(013) \mapsto \Delta_1(203)$  both create Möbius bands as vertex links of the vertices (0) and (2), respectively, and thus these 1-tetrahedron complexes cannot be subcomplexes of a 3-manifold triangulation.  $\Delta_1(013) \mapsto \Delta_1(230)$  and  $\Delta_1(013) \mapsto \Delta_1(302)$  both produce valid but isomorphic choices for  $\mathcal{T}_1$ : the minimal layered solid torus of type LST(1, 2, -3), Figure 8(ii). Lastly,  $\Delta_1(013) \mapsto \Delta_1(320)$  identifies the edge (03) with itself in reverse, it is hence invalid.

We discuss the two valid cases separately, starting with the latter one.



■ **Figure 8** The snapped 3-ball (i). A layered solid torus (ii), with four normal triangles comprising the single vertex link (iii), which is a triangulated hexagonal disk (iv).

► **Lemma 12.** *Let  $\mathcal{T}$  be a triangulation of a closed, orientable 3-manifold of treewidth one, with  $\mathcal{T}_1$  being a solid torus. Then  $\mathcal{T}$  triangulates a 3-manifold of Heegaard genus one.*

**Proof.** The proof consists of the following parts. **1.** We systematize all subcomplexes  $\mathcal{T}_2 \subset \mathcal{T}$  which arise from gluing a tetrahedron  $\Delta_2$  to  $\mathcal{T}_1$  along two triangular faces, and discard all complexes which cannot be part of a 3-manifold triangulation. **2.** We discuss the possible combinatorial types of subcomplexes  $\mathcal{T}_i$ ,  $i > 2$ , and triangulations of 3-manifolds arising from the remaining cases. **3.** We show for all resulting triangulations, that the fundamental group of the underlying manifold is, and is thus of Heegaard genus at most one.

To enumerate all possibilities for  $\mathcal{T}_2$ , assume, without loss of generality, that  $\mathcal{T}_1$  is obtained by  $\Delta_1(013) \mapsto \Delta_1(230)$ . The boundary  $\partial\mathcal{T}_1$  is built from two triangles  $(012)_\partial$  and  $(123)_\partial$ , sharing an edge (12), via the identifications  $(01) = (23)$  and  $(02) = (13)$ , see Figure 8(ii). The vertex link of  $\mathcal{T}_1$  is a triangulated hexagon as shown in Figure 8(iii)–(iv).

The second subcomplex  $\mathcal{T}_2$  is obtained from  $\mathcal{T}_1$  by gluing  $\Delta_2$  to the boundary of  $\mathcal{T}_2$  along two of its triangles. By symmetry, we are free to choose the first gluing. Hence, without loss of generality, let  $\mathcal{T}'_2$  be the complex obtained from  $\mathcal{T}_1$  by gluing  $\Delta_2$  to  $\mathcal{T}_1$  with gluing  $\Delta_2(012) \mapsto (012)_\partial$ . The result is a 2-vertex triangulated solid torus with four boundary triangles  $\Delta_2(013)$ ,  $\Delta_2(023)$ ,  $\Delta_2(123)$  and  $(123)_\partial$ , see Figure 9(ii). Since adjacent edges in the boundary of the unique vertex link of  $\mathcal{T}_1$  are always normal arcs in distinct triangles of  $\partial\mathcal{T}_1$ , the vertex links of  $\mathcal{T}'_2$  must be a triangulated 9-gon and a single triangle, see Figure 9(iii).

Note that both vertex links of  $\mathcal{T}'_2$  are symmetric with respect to the normal arcs coming from boundary triangles  $\Delta_2(013)$ ,  $\Delta_2(023)$  and  $\Delta_2(123)$ . By this symmetry, we are free to choose whether to glue  $\Delta_2(013)$ ,  $\Delta_2(023)$  or  $\Delta_2(123)$  to  $(123)_\partial$ , in order to obtain  $\mathcal{T}_2$ .

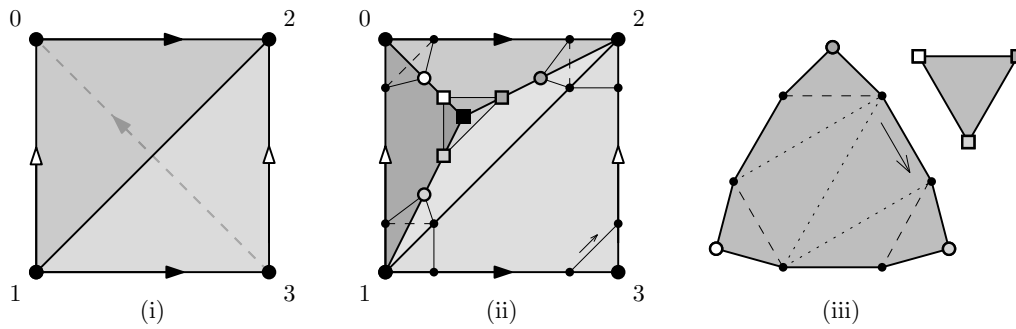


Figure 9 The solid torus  $\mathcal{T}_1$  (i), the complex  $\mathcal{T}_2'$  (ii), and the vertex links of  $\mathcal{T}_2'$  (iii).

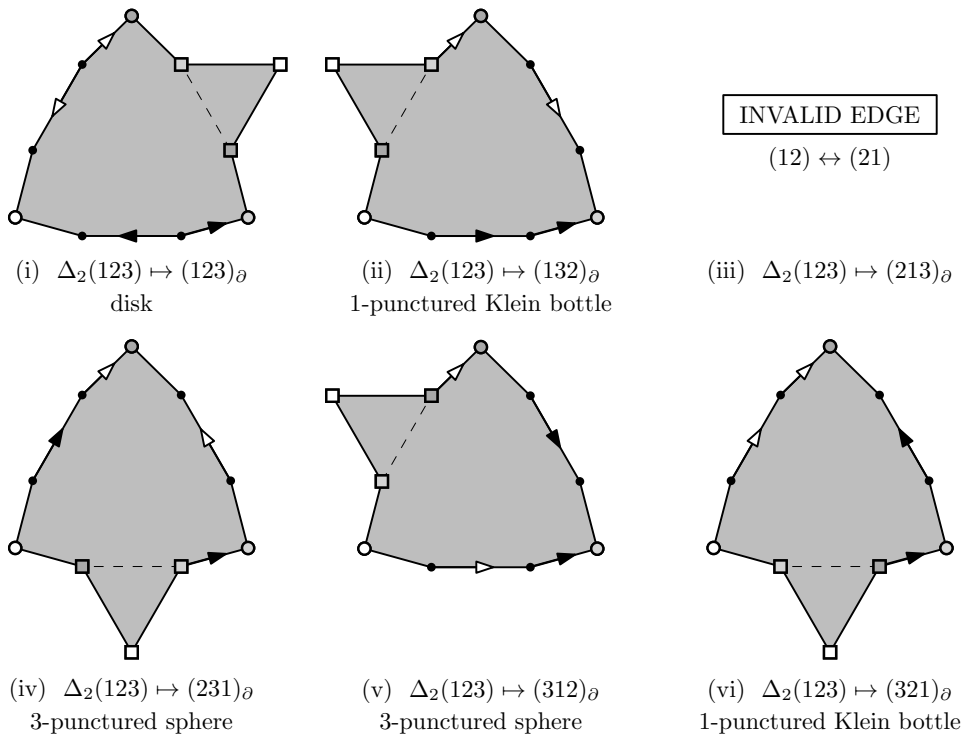


Figure 10

Therefore we have the following six possibilities to consider (Figure 10).

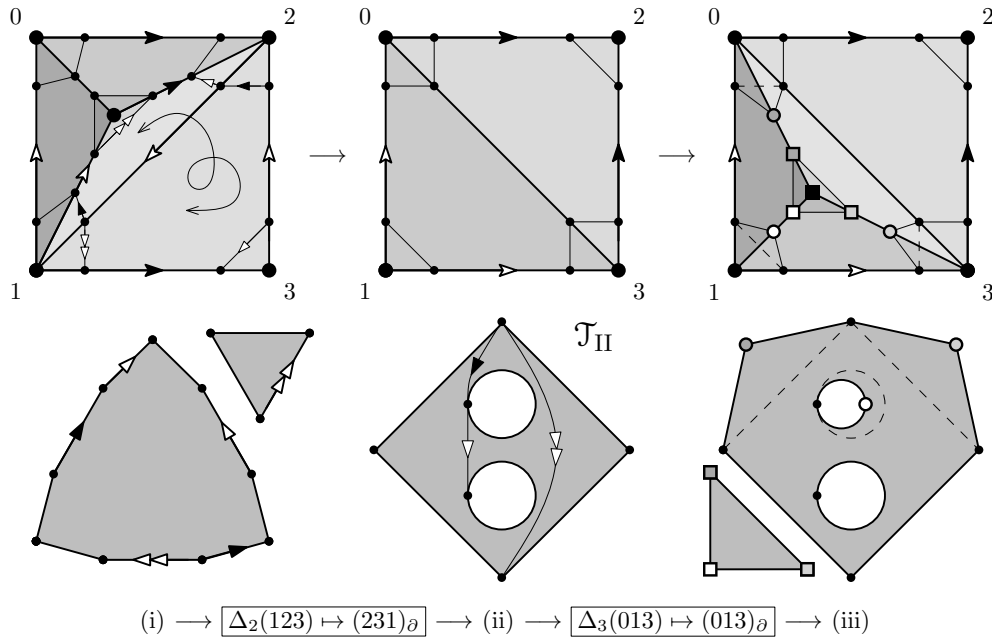
$\Delta_2(123) \mapsto (123)_\partial$  is a layering onto (12). It yields another layered solid torus with vertex link a triangulated hexagon with edges adjacent in the boundary of the link being normal arcs in distinct faces in  $\partial\mathcal{T}_2$ . Hence, in this case we have the same options for  $\mathcal{T}_3$  as the ones in this list. Any complex obtained by iterating this case is of this type.

Here, as well as for the remainder of this proof, whenever we obtain a subcomplex with all cases for the next subcomplex equal to a case already considered (i.e., isomorphic boundary complexes compatible with isomorphic boundaries of vertex links), we talk about these cases to be of the same *type*. We denote the one obtained via  $\Delta_2(123) \mapsto (123)_\partial$  by  $\mathcal{T}_1$ .

$\Delta_2(123) \mapsto (132)_\partial$  is invalid, as it creates a punctured Klein bottle as vertex link.

$\Delta_2(123) \mapsto (213)_\partial$  is invalid, as it identifies (12) on the boundary with itself in reverse.  
 $\Delta_2(123) \mapsto (231)_\partial$  results in a 1-vertex complex with triangles  $(013)_\partial$  and  $(023)_\partial$  comprising its boundary, which is isomorphic to the boundary of the snapped 3-ball with all of its three vertices identified. The vertex link is a 3-punctured sphere with two boundary components being normal loop arcs and one consisting of the remaining four normal arcs. This complex is discussed in detail below, and we denote its type by  $\mathcal{T}_{II}$ .  
 $\Delta_2(123) \mapsto (312)_\partial$  gives a 1-vertex complex of type  $\mathcal{T}_{II}$  as in the previous case.  
 $\Delta_2(123) \mapsto (321)_\partial$  is invalid: it produces a punctured Klein bottle in the vertex link.

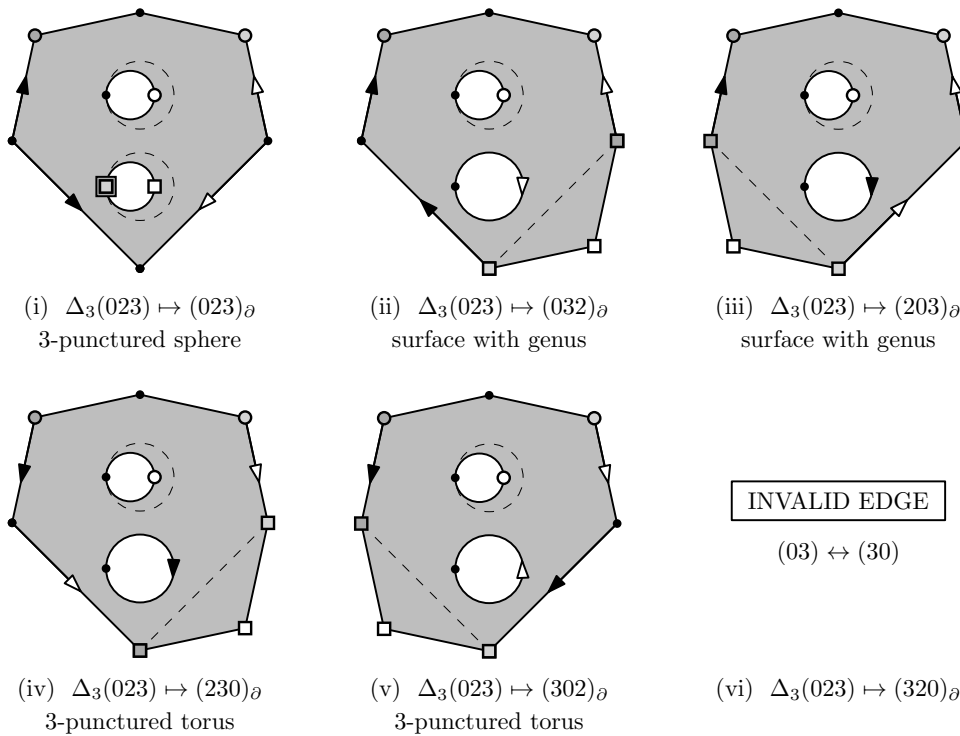
Now we discuss complexes of type  $\mathcal{T}_{II}$ . To this end, let  $\mathcal{T}_2$  be the complex in Figure 11(ii) defining this type. By gluing  $\Delta_3$  to  $\mathcal{T}_2$  along a boundary triangle, say  $\Delta_3(013) \mapsto (013)_\partial$ , we obtain a complex  $\mathcal{T}'_3$  (see Figure 11(iii)). Note that no boundary edge of the 3-punctured sphere vertex link  $\mathcal{L}$  can be identified with an edge in another boundary component of  $\mathcal{L}$ , for that would create genus in  $\mathcal{L}$  (an obstruction to being a subcomplex of a 3-manifold triangulation in which all vertex links must be  $\mathbb{S}^2$ ). As shown in Figure 12, there is a unique gluing to avoid this, namely  $\Delta_3(023) \mapsto (023)_\partial$ , which yields a 1-vertex complex  $\mathcal{T}_3$  with vertex link still being a 3-punctured sphere, but now with three boundary components consisting of two edges each, as indicated in Figure 12(i). Let  $\mathcal{T}_{III}$  denote its type. Repeating the same argument for  $\mathcal{T}_3$  implies that a valid  $\mathcal{T}_4$  must be again of type  $\mathcal{T}_{II}$ .



■ Figure 11

Altogether, the type of each intermediate complex  $\mathcal{T}_i$  ( $i < n$ ) is either  $\mathcal{T}_I$  (layered solid torus), or one of the two types  $\mathcal{T}_{II}$  and  $\mathcal{T}_{III}$  of 1-vertex complexes with a 3-punctured sphere as vertex link and boundary isomorphic to that of the snapped 3-ball with all vertices identified. If  $\mathcal{T}_{n-1}$  is of type  $\mathcal{T}_I$ , then it can always be completed to a triangulation of a closed 3-manifold by either adding a minimal layered solid torus or a snapped 3-ball. If  $\mathcal{T}_{n-1}$  is of type  $\mathcal{T}_{II}$  or  $\mathcal{T}_{III}$ , then it may be completed – if possible – by adding a snapped 3-ball.

To conclude that any resulting  $\mathcal{T}$  triangulates a 3-manifold of Heegaard genus at most one, first we observe that the fundamental group of  $\pi_1(\mathcal{T})$  is generated by one element.



■ **Figure 12**

Indeed,  $\pi_1(\mathcal{T}_1)$  is isomorphic to  $\mathbb{Z}$  and is generated by a boundary edge. Furthermore, since  $\mathcal{T}_1$  only has one vertex, all edges in  $\mathcal{T}_1$  must be loop edges, and no edge which is trivial in  $\pi_1(\mathcal{T}_1)$  can become non-trivial in the process of building up the triangulation of the closed 3-manifold. When we extend  $\mathcal{T}_1$  by attaching further tetrahedra along two triangles each, then either all edges of the newly added tetrahedron are identified with edges of the previous complex, or – in case of a layering – the unique new boundary edge can be expressed in terms of the existing generator. In both cases, the fundamental group of the new complex admits a presentation with one generator. Moreover, no new generator can arise from inserting a minimal layered solid torus or snapped 3-ball in the last step.

So either  $\pi_1(\mathcal{T})$  is infinite cyclic, i.e., isomorphic to  $\mathbb{Z}$ , in which case  $\mathcal{T}$  must be a triangulation of  $\mathbb{S}^2 \times \mathbb{S}^1$  [22]; or  $\pi_1(\mathcal{T})$  is finite, but then it is spherical by the Geometrization Theorem [40, p. 104], and thus must be a lens space [47, Theorem 4.4.14.(a)]. ◀

► **Lemma 13.** *Let  $\mathcal{T}$  be an  $n$ -tetrahedron triangulation of a closed, orientable 3-manifold of treewidth one, with both  $\mathcal{T}_1$  and  $\mathcal{T} \setminus \mathcal{T}_{n-1}$  being a snapped 3-ball. Then  $\mathcal{T}$  triangulates a 3-manifold of Heegaard genus one.*

The proof follows the same structure as the one of Lemma 12 (cf. [24]).

## 5 Some 3-manifolds of treewidth two

In what follows, we use the classification of 3-manifolds of treewidth one (Theorem 2) to show that a large class of orientable Seifert fibered spaces and some *graph manifolds* have treewidth two. This is done by exhibiting appropriate triangulations, which have all the hallmarks of a space station. First, we give an overview of the building blocks.

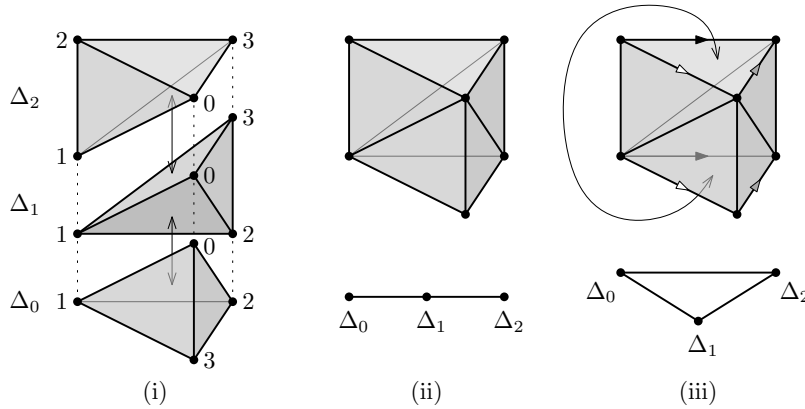
**Robotic arms.** These are just the layered triangulations of the solid torus with 2-triangle boundaries introduced in Section 3.2 and encountered in the proof of Theorem 2. Their dual graphs are thick paths, see Figure 3(v). A layered solid torus is of type  $LST(p, q, r)$  if its meridional disk intersects its boundary edges  $p, q$  and  $r$  times. For any coprime  $p, q, r$  with  $p + q + r = 0$ , a triangulation of type  $LST(p, q, r)$  can be realized by [10, Algorithm 1.2.17].

► **Example 14.** A special class of robotic arms are the ones of type  $LST(0, 1, 1)$ , as they can be used to trivially fill-in superfluous torus boundary components without inserting an unwanted exceptional fiber into a Seifert fibered space (cf. descriptions of  $\mathbb{A}_2$  and  $\mathbb{A}_1$  below). One of the standard triangulations of robotic arms of type  $LST(0, 1, 1)$  has three tetrahedra  $\Delta_i, 0 \leq i \leq 2$ , and is given by the gluing relations (4).

$$\begin{aligned} \Delta_0(023) &\mapsto \Delta_1(013), & \Delta_0(123) &\mapsto \Delta_1(120), & \Delta_1(023) &\mapsto \Delta_2(201), \\ \Delta_1(123) &\mapsto \Delta_2(301), & \Delta_2(023) &\mapsto \Delta_2(312). \end{aligned} \tag{4}$$

**Core unit with three docking sites.** Start with a triangle  $t$ , take the product  $t \times [0, 1]$ , triangulate it using three tetrahedra, Figure 13(i)–(ii), and glue  $t \times \{0\}$  to  $t \times \{1\}$  without a twist, Figure 13(iii). The dual graph of the resulting complex  $\mathbb{A}_3$  – topologically a solid torus – is  $K_3$ , hence of treewidth two. Its boundary – a 6-triangle triangulation of the torus – can be split into three 2-triangle annuli, corresponding to the edges of  $t$ , each of which we call a *docking site*. Edges running along a fiber and thus of type “vertex of base triangle cross circle” are termed *vertical edges*. Edges orthogonal to the fibers, i.e., the edges of  $t \times \{0\} = t \times \{1\}$ , are termed *horizontal edges*. The remaining edges are referred to as *diagonal edges*. More concisely, the triangulation of  $\mathbb{A}_3$  has gluing relations

$$\Delta_0(012) \mapsto \Delta_1(012), \quad \Delta_1(013) \mapsto \Delta_2(013), \quad \Delta_2(023) \mapsto \Delta_0(312). \tag{5}$$



■ **Figure 13** Construction of the core unit  $\mathbb{A}_3$  with three docking sites.

**Core assembly with  $r$  docking sites.** For  $r = 2$  (resp.  $r = 1$ ), take a core unit  $\mathbb{A}_3$  and glue a robotic arm of type  $LST(0, 1, 1)$  onto one (resp. two) of its docking sites such that the *unique boundary edge* of the robotic arm (i.e., the boundary edge which is only contained in one tetrahedron of the layered solid torus) is glued to a horizontal boundary edge of  $\mathbb{A}_3$  (see Example 14 for a detailed description of a particular triangulation of a layered solid torus of type  $LST(0, 1, 1)$  with unique boundary edge being  $\Delta_0(01)$ ). The resulting complex

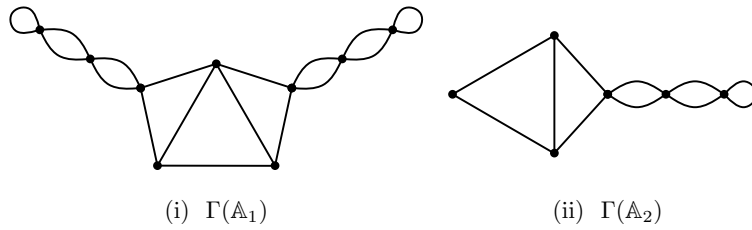


Figure 14

is denoted by  $\mathbb{A}_2$  (resp.  $\mathbb{A}_1$ ) and their dual graphs are shown in Figure 13. Observe that they have treewidth two.

For  $\mathbb{A}_r$  ( $r \geq 3$ ) take  $r - 2$  copies of  $\mathbb{A}_3$ , denote them by  $\mathbb{A}_3^i$ ,  $1 \leq i \leq r - 2$  with tetrahedra  $\Delta_0^i$ ,  $\Delta_1^i$  and  $\Delta_2^i$ ,  $1 \leq i \leq r - 2$ . Glue them together by mirroring them across one of their boundary components as shown by Equation (6) for  $1 \leq i \leq r - 3$  odd, and by Equation (7) for  $2 \leq i \leq r - 3$  even. See also Figure 15 on the top for the case  $r = 5$ .

The resulting complex, denoted by  $\mathbb{A}_r$ , has  $2r$  boundary triangles which become  $r$  2-triangle torus boundary components once identifications of vertical edges are introduced by gluing complexes with 2-triangle torus boundary components to them.

$$i \text{ odd: } \Delta_1^i(123) \mapsto \Delta_1^{i+1}(123), \quad \Delta_2^i(123) \mapsto \Delta_2^{i+1}(123). \tag{6}$$

$$i \text{ even: } \Delta_0^i(023) \mapsto \Delta_0^{i+1}(023), \quad \Delta_1^i(023) \mapsto \Delta_1^{i+1}(023). \tag{7}$$

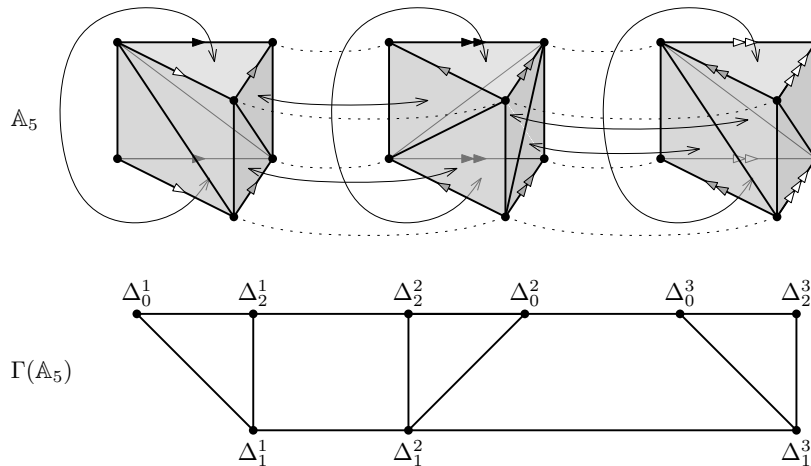
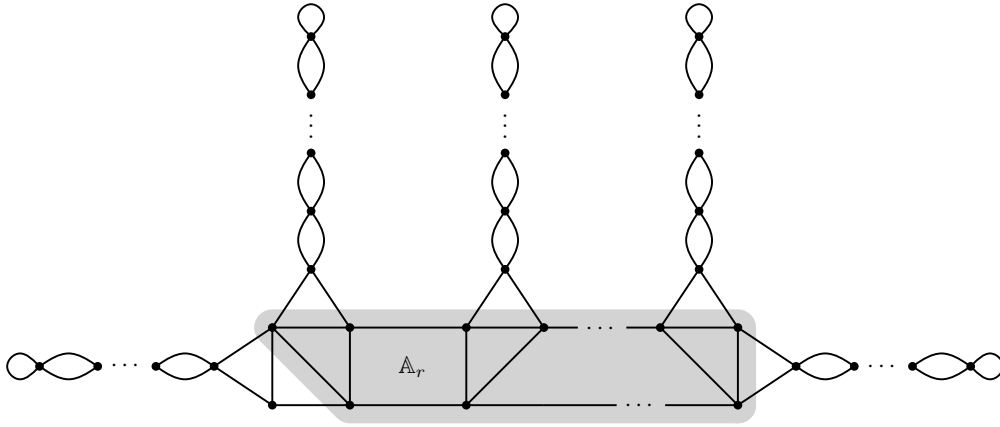


Figure 15

**Möbius laboratory module.** Such a complex, denoted by  $\mathbb{M}$ , is given by

$$\begin{aligned} T_0(123) \mapsto T_1(123), \quad T_0(023) \mapsto T_1(031), \quad T_1(012) \mapsto T_2(201) \\ T_1(023) \mapsto T_2(023), \quad T_0(013) \mapsto T_2(132). \end{aligned} \tag{8}$$

Its dual graph is a triangle with two double edges, and hence of treewidth two (see, for instance, Figure 17).  $\mathbb{M}$  has one torus boundary component given by the two triangles  $T_0(012)$  and  $T_2(013)$  with edges  $T_0(01) = T_2(13)$ ,  $T_0(02) = T_2(03)$ , and  $T_0(12) = T_2(01)$ .



■ **Figure 16** Dual graph of treewidth two triangulation of an orientable SFS over  $\mathbb{S}^2$ .

► **Theorem 15.** *Orientable Seifert fibered spaces over  $\mathbb{S}^2$  have treewidth at most two.*

**Proof.** To obtain a treewidth two triangulation of  $\text{SFS}[\mathbb{S}^2 : (a_1, b_1), \dots, (a_r, b_r)]$ , start with the core assembly  $\mathbb{A}_r$  and a collection of robotic arms  $\text{LST}(a_i, \pm|b_i|, -a_i \mp |b_i|)$ ,  $1 \leq i \leq r$ . The robotic arms are then glued to the  $r$  docking sites (2-triangle torus boundary components, separated by the vertical boundary edges) of  $\mathbb{A}_r$ , such that boundary edges of type  $a_i$  are glued to vertical boundary edges, and edges of type  $\pm|b_i|$  are glued to horizontal boundary edges. The sign in  $\text{LST}(a_i, \pm|b_i|, -a_i \mp |b_i|)$  is then determined by the type of diagonal edge in the  $i^{\text{th}}$  docking site of  $\mathbb{A}_r$  and by the sign of  $b_i$ . ◀

See Figure 16 for a picture of the dual graph of the resulting complex. It is of treewidth two. Note that, in some cases, a fibre of type  $(2, 1)$  can be realized by directly identifying the two triangles of a torus boundary component of  $\mathbb{A}_r$  with a twist. In the dual graph this then appears as a double edge rather than the attachment of a thick path. See Figure 18 on the right for an example in the treewidth two triangulation of the Poincaré homology sphere.

► **Theorem 16.** *An orientable SFS over a non-orientable surface is of treewidth at most two.*

**Proof.** To obtain a treewidth two triangulation of the orientable Seifert fibered space  $\text{SFS}[\mathcal{N}_g : (a_1, b_1), \dots, (a_r, b_r)]$  over the non-orientable surface  $\mathcal{N}_g$  of genus  $g$ , start with a core assembly  $\mathbb{A}_{r+g}$  and attach  $g$  copies  $\mathbb{M}_j$ ,  $1 \leq j \leq g$ , of the Möbius laboratory module via

$$T_0^j(012) \mapsto \Delta_2^j(201) \quad \text{and} \quad T_2^j(013) \mapsto \Delta_0^j(013), \tag{9}$$

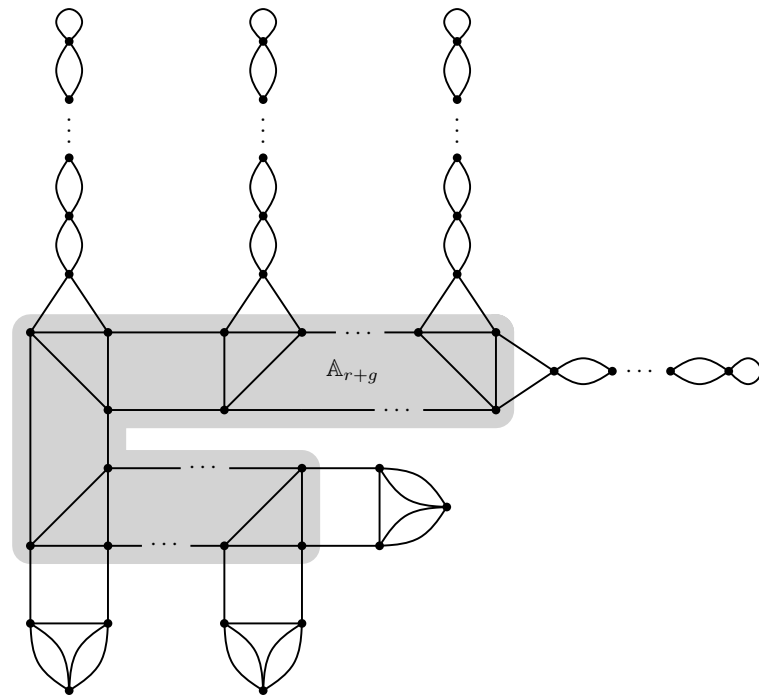
where  $T_0^j$ ,  $T_1^j$  and  $T_2^j$  are the tetrahedra comprising  $\mathbb{M}_j$ , and  $\Delta_0^j$ ,  $\Delta_1^j$  and  $\Delta_2^j$  denote the tetrahedra making up the first  $g$  core units (each being a copy of  $\mathbb{A}_3$ ) in  $\mathbb{A}_{r+g}$ .

Proceed by attaching a robotic arm of type  $\text{LST}(a_i, \pm|b_i|, -a_i \mp |b_i|)$ ,  $1 \leq i \leq r$ , to each of the remaining  $r$  docking sites. Again, for the gluings between the robotic arms and the core assembly  $\mathbb{A}_{r+g}$ , the edges of type  $a_i$  must be glued to the vertical boundary edges, the edges of type  $b_i$  must be glued to the horizontal boundary edges, and attention has to be paid to the signs of the  $b_i$  and to how exactly diagonal edges run. See Figure 17 for a picture of the dual graph of the resulting complex, which is of treewidth two by inspection. ◀

Combining Theorems 2, 15 and 16 immediately gives the following statement.

► **Corollary 17.** *An orientable Seifert fibered space  $\mathcal{M}$  over  $\mathbb{S}^2$  or a non-orientable surface is of treewidth one, if  $\mathcal{M}$  is a lens space or  $\text{SFS}[\mathbb{S}^2 : (2, 1), (2, 1), (2, -1)]$ , and two otherwise.*





■ **Figure 17** Dual graph of a treewidth two triangulation of an orientable SFS over  $\mathcal{N}_g$ .

► **Corollary 18.** *Orientable spherical or “ $\mathbb{S}^2 \times \mathbb{R}$ ” 3-manifolds are of treewidth at most two.*

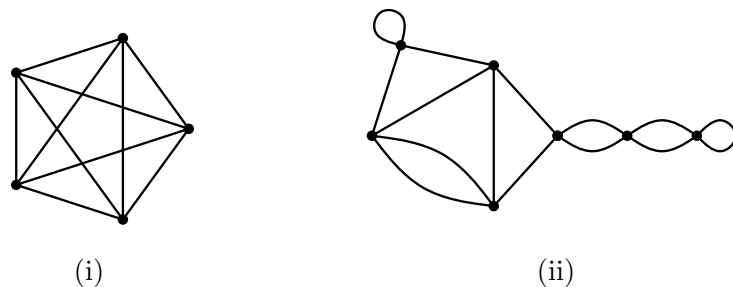
This follows directly from Theorems 15 and 16, see also [24].

► **Corollary 19.** *Graph manifolds  $\mathcal{M}_T$  modeled on a tree  $T$  with nodes being orientable Seifert fibered spaces over  $\mathbb{S}^2$  or  $\mathcal{N}_g$ ,  $g > 0$ , have treewidth at most two.*

See [24] for a proof of this statement and an example.

► **Corollary 20.** *Minimal triangulations are not always of minimum treewidth.*

**Proof.** The Poincaré homology sphere  $\Sigma^3 = \text{SFS}[\mathbb{S}^2 : (2, 1), (3, 1), (5, -4)]$  has treewidth two but its minimal triangulation has treewidth four, see Figure 18. ◀



■ **Figure 18** Dual graph of the minimal (i), and of a treewidth two (ii) triangulation of  $\Sigma^3$ .

► **Corollary 21.** *There exist irreducible 3-manifolds with treewidth two, but arbitrarily high Heegaard genus.*

This now follows from [9, Theorem 1.1 (i)], see the full version [24] for a proof.

Using Theorems 2, 15 and 16 we can now determine the treewidth of most of the 3-manifolds from the 10-tetrahedra census, see Table 1.

■ **Table 1** The 4979 3-manifolds triangulable with  $\leq 10$  tetrahedra and their treewidths.

$n$	# mfd. $M$	$\text{tw}(M) = 0$	$\text{tw}(M) = 1$	$\text{tw}(M) = 2$	unknown
1	3	3	0	0	0
2	7	0	7	0	0
3	7	0	6	1	0
4	14	0	10	4	0
5	31	0	20	11	0
6	74	0	36	36	2
7	175	0	72	100	3
8	436	0	136	297	3
9	1154	0	272	861	21
10	3078	0	528	2489	61
$\Sigma$	4979	3	1087	3799	90

► **Remark 22.** Using similar constructions it can be shown that orientable Seifert fibered spaces over orientable surfaces have treewidth at most four. However, since this only provides an upper bound rather than determining the treewidth of some family of 3-manifolds, we refer the reader to the full version of this article for a detailed description of these triangulations.

---

## References

- 1 D. Bachman, R. Derby-Talbot, and E. Sedgwick. Computing Heegaard genus is NP-hard. In M. Loebli, J. Nešetřil, and R. Thomas, editors, *A Journey Through Discrete Mathematics: A Tribute to Jiří Matoušek*, pages 59–87. Springer, 2017. doi:10.1007/978-3-319-44479-6.
- 2 M. C. Bell. *Recognising mapping classes*. PhD thesis, University of Warwick, June 2015. URL: <https://wrap.warwick.ac.uk/77123>.
- 3 L. Bessières, G. Besson, S. Maillot, M. Boileau, and J. Porti. *Geometrisation of 3-manifolds*, volume 13 of *EMS Tracts in Mathematics*. European Mathematical Society (EMS), Zürich, 2010. doi:10.4171/082.
- 4 R. H. Bing. An alternative proof that 3-manifolds can be triangulated. *Ann. of Math. (2)*, 69:37–65, 1959. doi:10.2307/1970092.
- 5 H. L. Bodlaender. A Tourist Guide through Treewidth. *Acta Cybern.*, 11(1-2):1–21, 1993. URL: [https://www.inf.u-szeged.hu/actacybernetica/edb/vol11n1\\_2/Bodlaender\\_1993\\_ActaCybernetica.xml](https://www.inf.u-szeged.hu/actacybernetica/edb/vol11n1_2/Bodlaender_1993_ActaCybernetica.xml).
- 6 H. L. Bodlaender. A Partial  $k$ -Arboretum of Graphs with Bounded Treewidth. *Theor. Comput. Sci.*, 209(1-2):1–45, 1998. doi:10.1016/S0304-3975(97)00228-4.
- 7 H. L. Bodlaender. Discovering Treewidth. In *SOFSEM 2005: Theory and Practice of Computer Science, 31st Conference on Current Trends in Theory and Practice of Computer Science, Liptovský Ján, Slovakia, January 22–28, 2005, Proceedings*, pages 1–16, 2005. doi:10.1007/978-3-540-30577-4\_1.
- 8 H. L. Bodlaender and A. M. C. A. Koster. Combinatorial Optimization on Graphs of Bounded Treewidth. *Comput. J.*, 51(3):255–269, 2008. doi:10.1093/comjnl/bxm037.

- 9 M. Boileau and H. Zieschang. Heegaard genus of closed orientable Seifert 3-manifolds. *Invent. Math.*, 76(3):455–468, 1984. doi:10.1007/BF01388469.
- 10 B. A. Burton. *Minimal triangulations and normal surfaces*. PhD thesis, University of Melbourne, September 2003. URL: <https://people.smp.uq.edu.au/BenjaminBurton/papers/2003-thesis.html>.
- 11 B. A. Burton. Computational topology with Regina: algorithms, heuristics and implementations. In *Geometry and topology down under*, volume 597 of *Contemp. Math.*, pages 195–224. Amer. Math. Soc., Providence, RI, 2013. doi:10.1090/conm/597/11877.
- 12 B. A. Burton, R. Budney, W. Pettersson, et al. Regina: Software for low-dimensional topology, 1999–2017. URL: <https://regina-normal.github.io>.
- 13 B. A. Burton and R. G. Downey. Courcelle’s theorem for triangulations. *J. Comb. Theory, Ser. A*, 146:264–294, 2017. doi:10.1016/j.jcta.2016.10.001.
- 14 B. A. Burton, T. Lewiner, J. Paixão, and J. Spreer. Parameterized Complexity of Discrete Morse Theory. *ACM Trans. Math. Softw.*, 42(1):6:1–6:24, 2016. doi:10.1145/2738034.
- 15 B. A. Burton, C. Maria, and J. Spreer. Algorithms and complexity for Turaev–Viro invariants. *J. Appl. Comput. Topol.*, 2(1–2):33–53, 2018. doi:10.1007/s41468-018-0016-2.
- 16 B. A. Burton and J. Spreer. The complexity of detecting taut angle structures on triangulations. In *Proceedings of the Twenty-Fourth Annual ACM-SIAM Symposium on Discrete Algorithms, SODA 2013, New Orleans, Louisiana, USA, January 6–8, 2013*, pages 168–183, 2013. doi:10.1137/1.9781611973105.13.
- 17 A. de Mesmay, J. Purcell, S. Schleimer, and E. Sedgwick. On the tree-width of knot diagrams, 2018. 13 pages, 4 figures. arXiv:1809.02172.
- 18 J. Díaz, J. Petit, and M. J. Serna. A survey of graph layout problems. *ACM Comput. Surv.*, 34(3):313–356, 2002. doi:10.1145/568522.568523.
- 19 R. Diestel. *Graph theory*, volume 173 of *Graduate Texts in Mathematics*. Springer, Berlin, fifth edition, 2017. doi:10.1007/978-3-662-53622-3.
- 20 R. G. Downey and M. R. Fellows. *Fundamentals of parameterized complexity*. Texts in Computer Science. Springer, London, 2013. doi:10.1007/978-1-4471-5559-1.
- 21 R. S. Hamilton. Three-manifolds with positive Ricci curvature. *J. Differential Geom.*, 17(2):255–306, 1982. doi:10.4310/jdg/1214436922.
- 22 A. Hatcher. Notes on Basic 3-Manifold Topology, 2007. URL: <https://pi.math.cornell.edu/~hatcher/3M/3Mfds.pdf>.
- 23 J. Hempel. *3-manifolds*. AMS Chelsea Publishing, Providence, RI, 2004. Reprint of the 1976 original. doi:10.1090/chel/349.
- 24 K. Huszár and J. Spreer. 3-Manifold triangulations with small treewidth, 2018. 34 pages, 30 figures, 1 table. arXiv:1812.05528.
- 25 K. Huszár, J. Spreer, and U. Wagner. On the treewidth of triangulated 3-manifolds, 2017. 25 pages, 6 figures, 1 table. An extended abstract of this paper appeared in the Proceedings of the 34th International Symposium on Computational Geometry (SoCG 2018), Budapest, June 11–14 2018. arXiv:1712.00434.
- 26 W. Jaco. *Lectures on three-manifold topology*, volume 43 of *CBMS Regional Conference Series in Mathematics*. American Mathematical Society, Providence, R.I., 1980. doi:10.1090/cbms/043.
- 27 W. Jaco and J. H. Rubinstein. Layered-triangulations of 3-manifolds, 2006. 97 pages, 32 figures. arXiv:math/0603601.
- 28 B. Kleiner and J. Lott. Notes on Perelman’s papers. *Geom. Topol.*, 12(5):2587–2855, 2008. doi:10.2140/gt.2008.12.2587.
- 29 L. Lovász. Graph minor theory. *Bull. Amer. Math. Soc. (N.S.)*, 43(1):75–86, 2006. doi:10.1090/S0273-0979-05-01088-8.
- 30 F. H. Lutz. Triangulated Manifolds with Few Vertices: Geometric 3-Manifolds, 2003. 48 pages, 18 figures. arXiv:math/0311116.
- 31 C. Maria and J. Purcell. Treewidth, crushing, and hyperbolic volume, 2018. 20 pages, 12 figures. arXiv:1805.02357.

- 32 C. Maria and J. Spreer. A polynomial time algorithm to compute quantum invariants of 3-manifolds with bounded first Betti number. In *Proceedings of the Twenty-Eighth Annual ACM-SIAM Symposium on Discrete Algorithms, SODA 2017, Barcelona, Spain, Hotel Porta Fira, January 16–19*, pages 2721–2732, 2017. doi:10.1137/1.9781611974782.180.
- 33 J. Milnor. Towards the Poincaré conjecture and the classification of 3-manifolds. *Notices Amer. Math. Soc.*, 50(10):1226–1233, 2003.
- 34 E. E. Moise. Affine structures in 3-manifolds. V. The triangulation theorem and Hauptvermutung. *Ann. of Math. (2)*, 56:96–114, 1952. doi:10.2307/1969769.
- 35 J. M. Montesinos. *Classical tessellations and three-manifolds*. Universitext. Springer-Verlag, Berlin, 1987. doi:10.1007/978-3-642-61572-6.
- 36 P. Orlik. *Seifert manifolds*, volume 291 of *Lecture Notes in Mathematics*. Springer-Verlag, Berlin-New York, 1972. doi:10.1007/BFb0060329.
- 37 G. Perelman. The entropy formula for the Ricci flow and its geometric applications, 2002. 39 pages. arXiv:math/0211159.
- 38 G. Perelman. Finite extinction time for the solutions to the Ricci flow on certain three-manifolds, 2003. 7 pages. arXiv:math/0307245.
- 39 G. Perelman. Ricci flow with surgery on three-manifolds, 2003. 22 pages. arXiv:math/0303109.
- 40 J. Porti. Geometrization of three manifolds and Perelman’s proof. *Rev. R. Acad. Cienc. Exactas Fís. Nat. Ser. A Math. RACSAM*, 102(1):101–125, 2008. doi:10.1007/BF03191814.
- 41 N. Robertson and P. D. Seymour. Graph Minors. II. Algorithmic Aspects of Tree-Width. *J. Algorithms*, 7(3):309–322, 1986. doi:10.1016/0196-6774(86)90023-4.
- 42 N. Saveliev. *Lectures on the topology of 3-manifolds*. De Gruyter Textbook. Walter de Gruyter & Co., Berlin, 2nd edition, 2012. doi:10.1515/9783110250367.
- 43 M. Scharlemann. Heegaard splittings of compact 3-manifolds. In *Handbook of geometric topology*, pages 921–953. North-Holland, Amsterdam, 2002. doi:10.1016/B978-044482432-5/50019-6.
- 44 J. Schultens. *Introduction to 3-manifolds*, volume 151 of *Graduate Studies in Mathematics*. Amer. Math. Soc., Providence, RI, 2014. doi:10.1090/gsm/151.
- 45 P. Scott. The geometries of 3-manifolds. *Bull. London Math. Soc.*, 15(5):401–487, 1983. doi:10.1112/blms/15.5.401.
- 46 H. Seifert. Topologie Dreidimensionaler Gefaserner Räume. *Acta Math.*, 60(1):147–238, 1933. doi:10.1007/BF02398271.
- 47 W. P. Thurston. Three-dimensional manifolds, Kleinian groups and hyperbolic geometry. *Bull. Amer. Math. Soc. (N.S.)*, 6(3):357–381, 1982. doi:10.1090/S0273-0979-1982-15003-0.
- 48 W. P. Thurston. *Three-dimensional geometry and topology. Vol. 1*, volume 35 of *Princeton Mathematical Series*. Princeton University Press, Princeton, NJ, 1997. Edited by S. Levy. doi:10.1515/9781400865321.